
CAUSAL DISCOVERY AND CLASSIFICATION USING LEMPEL-ZIV COMPLEXITY

Dhruthi

Department of Computer Science and Information Systems
BITS Pilani K K Birla Goa Campus
403726, Goa, India
f20231019@goa.bits-pilani.ac.in

Nithin Nagaraj

Complex Systems Programme
National Institute of Advanced Studies, Indian Institute of Science Campus
Bengaluru, 560012, Karnataka, India
nithin@nias.res.in

Harikrishnan N B

Department of Computer Science and Information Systems
BITS Pilani K K Birla Goa Campus
403726, Goa, India
harikrishnannb@goa.bits-pilani.ac.in

ABSTRACT

Inferring causal relationships in the decision-making processes of machine learning algorithms is a crucial step toward achieving explainable Artificial Intelligence (AI). In this research, we introduce a novel causality measure and a distance metric derived from Lempel-Ziv (LZ) complexity. We explore how the proposed causality measure can be used in decision trees by enabling splits based on features that most strongly *cause* the outcome. We further evaluate the effectiveness of the causality-based decision tree and the distance-based decision tree in comparison to a traditional decision tree using Gini impurity. While the proposed methods demonstrate comparable classification performance overall, the causality-based decision tree significantly outperforms both the distance-based decision tree and the Gini-based decision tree on datasets generated from causal models. This result indicates that the proposed approach can capture insights beyond those of classical decision trees, especially in causally structured data. Based on the features used in the LZ causal measure based decision tree, we introduce a causal strength for each features in the dataset so as to infer the predominant causal variables for the occurrence of the outcome.

Keywords Lempel-Ziv Complexity · Decision Tree · Causal Discovery · Machine Learning

Incorporating causal based explanation to Machine Learning (ML) decision making process is an integral part of trustworthiness and model explainability [1]. In many scenario's a dataset dealt by an ML scientist would be observational data. Observational data are historical records of a phenomenon observed passively. An example of observational data would be studying the link between smoking and lung cancer. Such a study includes the documentation of the historical recording of the smoking/non-smoking habits and health condition over time. It is essential to note that such studies do not ask people to start and quit smoking. On the other hand, interventional data includes design experiments to study the effect of a specific variable through randomized control trials (RCT's) [2]. For eg., in the COVID -19 vaccine trials, researchers do interventional study to establish the causal influence of a proposed treatment for a desired outcome through RCT's. In several cases, conducting RCT's is not feasible due to ethical reasons. So, it is essential to have robust methods that can give causal explanation from observational data. There are several methods used to

detect causal directions from observational data. The methods like Granger Causality, [3] (GC), Transfer Entropy [4] (TE) make use of Norbert Wiener’s notion of causality [5]. Wiener’s definition of Causality states – *if a time series X causes a time series Y , then past values of X should contain information that help predict Y above and beyond the information contained in past values of Y alone* [6]. The above definition of predictability as an indicative measure for causality is expanded to incorporate compressibility as they are related. The following methods uses compressibility as an causality indicative measure: Compression Complexity Causality [7], ORIGO [8], ERGO [9]. ORIGO is a causal discovery method based on minimum description length principle (MDL). ORIGO infers that X is likely a cause of Y if compressing X first, followed by compressing Y given X , results in better compression than doing it in the reverse order [8]. ERGO relies on complexity estimates as proxies for Kolmogorov complexity instead lossless compression [9]. In [10], the authors introduced a penalty and efficacy formulation utilizing Lempel-Ziv (LZ) complexity and Effort to Compress (ETC) to develop a new causality measure. This method was evaluated on various datasets, including an autoregressive (AR) process, the Tuebingen datasets [11], and SARS-CoV-2 viral genome datasets. The performance of their approach was compared with that of state-of-the-art methods, specifically ORIGO and ERGO. The results from all experiments conducted in [10] demonstrated that the proposed LZ and ETC-based causality measures perform competitively against these established techniques on synthetic benchmarks.

The aim of this research is to develop novel causal direction identifying measure from univariate datasets, and incorporate in decision tree algorithm for developing a causally informed model. The steps undertaken to achieve the goals are as follows:

1. Novel causal measure based on Lempel-Ziv (LZ) Complexity - Inspired by the efficacy of the compression complexity based causality measures, we propose a novel causality testing measure based on Lempel-Ziv complexity to check the direction of causation from univariate temporal/non-temporal data. The proposed method differs significantly from the Lempel-Ziv and ETC-based causality measures introduced in [10]. We demonstrate a use case where our approach outperforms the causality measure suggested in the above paper.
2. Testing of the causality measure - Test the efficacy of the causality measure in real world and synthetic datasets.
3. Integration of the proposed causal measure in ML decision tree model - we integrate the proposed measure into a decision tree as a splitting criterion, creating a tree whose decisions at each node are guided by our proposed causality measure.
4. Novel distance metric derived from Lempel-Ziv complexity - introduced a novel distance metric derived from the Lempel-Ziv complexity measure, which is incorporated into the decision tree.
5. Performance comparison - compare the two proposed methods with a decision tree that uses the classical *Gini impurity* on several datasets, including *AR dataset, Iris, Breast Cancer, Voting, Car Evaluation, KRKPA7, Mushroom, Thyroid, Heart Disease*.
6. Interpretability of our proposed model: We propose a *feature importance score* based on LZ causal measure based decision tree. This score will rank the features based on its causal influence on the outcome variable.

The sections in the paper are arranged as follows: Section 1 describes the proposed method, the experiments on validating the LZ based causal measure using synthetic dataset and incorporating LZ based causal and distance measure with decision trees is highlighted in Section 2. In Section 3, we provide the Conclusion. The appendix material can be accessed in Section 4.

1 Proposed Method

In this section, we describe the proposed causality and distance based measure derived from Lempel-Ziv complexity. The proposed causality measure has the following assumptions:

1. Assumption 1: Cause happens either before the effect or they occur together. We don’t consider retrocausal scenarios in this study.
2. Assumption 2: There is no confounding variable that causes X and Y , where X and Y are temporal/non-temporal data.

Consider two univariate dataset $X = [a, b, c, a, c, b, a, a, \dots]$ and $Y = [b, a, a, a, b, c, \dots]$ which may or may not have temporal structure. We want to develop a measure using which we want to comment the direction causality. i.e., $X \rightarrow Y$ or $Y \rightarrow X$. We want the measure to have the following properties:

- If $X \rightarrow Y$, then the grammar of X constructed over real time has patterns that better explain Y . The extra penalty incurred by explaining Y using the generated grammar of X denoted as $LZ - P_{X \rightarrow Y}$ is less compared

to the penalty incurred by explaining X using the generated grammar of Y denoted as $LZ - P_{Y \rightarrow X}$. For this case, $LZ - P_{X \rightarrow Y} < LZ - P_{Y \rightarrow X}$. The inequality will be reversed if $Y \rightarrow X$.

- Explaining X using the real time generated grammar of X denoted as $LZ - P_{X \rightarrow X}$ should give zero penalty. This follows from the assumption 1.

We now describe the construction of the real time grammar of a temporal/ non-temporal data for the proposed causality measure.

1.1 Causality Measure based on Lempel-Ziv Complexity

1.1.1 Definition

Given two symbolic sequences, $x = x_0x_1x_2\dots x_m$ and $y = y_0y_1y_2\dots y_n$, such that $0 \leq x_k \leq m-1$ and $0 \leq y_k \leq n-1$, we define $LZ - P_{x \rightarrow y}$ as the penalty incurred by explaining y using the real time grammar of x . The algorithm for calculating the penalty is described in Algorithm 1. For example, consider the two strings $x = "101110"$ and $y = "110111"$. Then $LZ - P_{x \rightarrow y}$ is calculated according to the following steps:

- **Step 0:** We consider the two strings x and y , and construct their respective grammar sets G_x and G_y respectively using the Lempel-Ziv algorithm. We monitor the overlap at each stage, which can be thought to represent the extent to which the current and previous values of x influence y .

$$x = 101110, \quad y = 110111, \quad \text{overlap} = 0, \quad G_x = \phi, \quad G_y = \phi.$$

- **Step 1:** Since we are inferring the strength of causation from string x to string y , we start with the selection of the smallest substring of x , starting from the first index, that is not already present in its grammar set. Since the grammar set is empty, '1' is selected and added to G_x .

$$x = \underline{1}01110, \quad \text{overlap} = 0, \quad G_x = \{ '1' \}, \quad G_y = \phi.$$

- **Step 2:** Similarly, for string y , the substring '1' is selected. Since this substring is already present in G_x , overlap is incremented. We can interpret this as the '1' present in x inducing its occurrence in y .

$$y = \underline{1}10111, \quad \text{overlap} = 1, \quad G_x = \{ '1' \}, \quad G_y = \{ '1' \}.$$

- **Step 3:** The process is now repeated. The starting index of the subsequent substring must immediately follow the terminal index of the preceding substring, so that no information is lost. Hence '0' is selected and added to the set G_x .

$$x = \underline{10}1110, \quad \text{overlap} = 1, \quad G_x = \{ '1', '0' \}, \quad G_y = \{ '1' \}.$$

- **Step 4:** As in Step 3, we consider the smallest subsequently occurring substring, '1'. Since it is already present in G_y , we consider the substring '10' instead. '10' is not present in G_y and is hence added to it, and since it is not present in G_x , overlap is not incremented.

$$y = \underline{110}111, \quad \text{overlap} = 1, \quad G_x = \{ '1', '0' \}, \quad G_y = \{ '1', '10' \}.$$

- **Step 5:** The substring '1' is already present in G_x . The substring '11' is selected and added to G_x , as in Step 3.

$$x = 10\underline{11}10, \quad \text{overlap} = 1, \quad G_x = \{ '1', '0', '11' \}, \quad G_y = \{ '1', '10' \}.$$

- **Step 6:** The substring '1' is already present in G_y . The substring '11' is selected and added to G_y . Since it is already present in G_x , overlap is incremented.

$$y = 110\underline{11}1, \quad \text{overlap} = 2, \quad G_x = \{ '1', '0', '11' \}, \quad G_y = \{ '1', '10', '11' \}.$$

- **Step 7:** The substring '10' is not present in G_x , and is hence added to G_x .

$$x = 1011\underline{10}, \quad \text{overlap} = 2, \quad G_x = \{ '1', '0', '11', '10' \}, \quad G_y = \{ '1', '10', '11' \}.$$

Since there are no more substrings left in either string that can be added to the respective grammar sets, the process stops here, and $LZ - P_{x \rightarrow y}$ is found to be $(|G_y| - \text{overlap})$, which is 1. In the same manner, $LZ - P_{y \rightarrow x}$ is also found to be 1.

If $LZ - P_{x \rightarrow y} < LZ - P_{y \rightarrow x}$, we can say that x causes y . Similarly, if $LZ - P_{y \rightarrow x} < LZ - P_{x \rightarrow y}$, we conclude that y causes x . In this case, since the penalties are equal, the flow of information between y and x is bidirectional and we decide the direction of causation by a coin flip.

In the upcoming section 2, we test the correctness of the proposed causality measure for determining the direction of causation from univariate datasets.

Algorithm 1 Calculation of Penalty of a string y of length n given another string x of length m

```

1: Input: String  $y$  of length  $n$ , String  $x$  of length  $m$ .
2: Output: Penalty of using  $x$  to compress  $y$ 
3: Initialize set  $G_x \leftarrow \emptyset$  {Empty grammar set}
4: Initialize set  $G_y \leftarrow \emptyset$  {Empty grammar set}
5: Initialize  $i_x \leftarrow 1$ 
6: Initialize  $i_y \leftarrow 1$ 
7: Initialize  $overlap \leftarrow 0$ 
8: while  $i_y \leq n$  do
9:   if  $i_x \leq m$  then
10:    Set  $j_x \leftarrow i_x$ 
11:    while  $x[i_x : j_x] \in G_x$  and  $j_x < m$  do
12:      Increase  $j_x$  by 1
13:    end while
14:    Add substring  $x[i : j]$  to  $G_x$ 
15:  end if
16:  Set  $j_y \leftarrow i_y$ 
17:  while  $y[i_y : j_y] \in G_y$  and  $j < n$  do
18:    Increase  $j_y$  by 1
19:  end while
20:  if  $y[i_y : j_y] \in G_x$  then
21:    Increase  $overlap$  by 1
22:  end if
23:  Add  $y[i_y : j_y]$  to  $G_y$ 
24:  Set  $i_x \leftarrow j_x + 1$ 
25:  Set  $i_y \leftarrow j_y + 1$ 
26: end while
27: return  $|G_y| - overlap$ 

```

1.2 A Distance metric based on Lempel-Ziv Complexity

In this section, we define the a distance metric derived from the grammar of two symbolic sequences. The grammar construction is based on Lempel-Ziv algorithm [12]. Given two symbolic sequences, $x = x_0x_1x_2\dots x_m$ and $y = y_0y_1y_2\dots y_n$, such that $0 \leq x_k \leq m - 1$ and $0 \leq y_k \leq n - 1$, their grammars G_x and G_y respectively can be encoded using the Lempel-Ziv Algorithm, as shown in Algorithm 2. The Lempel-Ziv distance between two sets G_x and G_y is

$$d_{LZ}(G_x, G_y) = |G_x/G_y| + |G_y/G_x|, \quad (1)$$

where $|G|$ represents the cardinality of a set G . The proof of the given measure being a distance metric on the metric space of the power set of set of all symbolic sequences of all finite lengths is given in Appendix 4.1. Decision trees utilizing this metric select thresholds depending on the symbolic sequence structure, and are thus sensitive to the permutation of training data.

Algorithm 2 Calculation of Grammar of a String Using Lempel-Ziv Complexity

```

1: Input: String  $x$  of length  $n$ 
2: Output: Grammar of the string,  $G_x$ 
3: Initialize set  $G_x \leftarrow \emptyset$  {Empty grammar set}
4: Initialize  $i \leftarrow 1$ 
5: while  $i \leq n$  do
6:   Set  $j \leftarrow i$ 
7:   while  $x[i : j] \in G_x$  and  $j < n$  do
8:     Increase  $j$  by 1
9:   end while
10:  Add substring  $x[i : j]$  to  $G_x$ 
11:  Set  $i \leftarrow j + 1$ 
12: end while
13: return  $G_x$ 

```

1.3 Applicability in Decision Trees

In this section, we highlight on the utilization of the proposed causality and distance measure as a splitting criteria in decision tree thereby yielding (a) Lempel-Ziv Causal Measure based decision tree, (b) Lempel-Ziv distance metric based decision tree.

1.3.1 Utilization as a splitting criteria

To split a binary tree at a given node, a feature and threshold are selected based on minimizing LZ -based causality measure between a feature string (for a particular chosen threshold) and target string. Each feature and target value is transformed into symbolic sequences: elements in the feature column are represented as 0 if below the threshold, and 1 if above. In the target symbolic sequence y , a given label l is represented as 1 and all others as 0. The feature and threshold selection is done as per the following equation:

$$(best\ feature, best\ threshold) = \arg \min_{feature, target, label} (LZ - P_{feature \rightarrow target}). \quad (2)$$

A similar approach is utilized to implement a LZ -distance based decision tree, now replacing the LZ -P causality measure with the LZ -based distance measure as defined in Section 1.2. Once the symbolic sequences are found, algorithm 2 is utilized to find the grammar of the symbolic sequences, represented by $G_{feature}$ and G_{target} respectively. The feature, threshold pair with minimum distance with respect to the target label is selected, based on the following equation.

$$(best\ feature, best\ threshold) = \arg \min_{feature, target, label} (d_{LZ}(G_{feature}, G_{target})). \quad (3)$$

1.3.2 Causal Strength of a feature on a target

We propose a method of ranking of the strength of causation of different attributes on a particular label based on the causal decision tree. Consider a decision tree with m nodes, and d_i denotes the depth of the i th node. The causal strength s_j for a feature j to the target is given by the following formulation:

$$s_j = \sum_{i=0}^m a_{ij} \cdot 2^{-d_i}, \quad \text{where } a_{ij} = \begin{cases} 1 & \text{if } j \text{ is the splitting feature at the } i\text{th node,} \\ 0 & \text{otherwise} \end{cases} \quad (4)$$

These scores can then be normalized. This provides a relative ranking of causal influence of the features on the target attribute.

2 Experiments

In this section, we first demonstrate the efficacy of the proposed causal measure in successfully determining the direction of causation for coupled Auto Regressive (AR) processes, coupled logistic map as described in section 2.1 and section 2.2 respectively. We also compare the performance of proposed method with penalty measure defined in [10] for real world dataset obtained from Tuebingen cause-effect pairs repository¹ as mentioned in Section 2.3. The integration of the proposed causal measure and distance based measure with decision trees and its performance comparison with decision tree based on gini impurity for the following datasets *AR dataset*, *Iris*, *Breast Cancer*, *Voting*, *Car Evaluation*, *KRKA7*, *Mushroom*, *Thyroid*, *Heart Disease*.

2.1 Simple causation in AR processes of various orders

Data was generated from a coupled auto regressive process of order $p = 1, 5, 20, 100$. The governing equation for $X(t)$ and $Y(t)$, where both are timeseries data are as follows:

$$X(t) = aX(t-1) + \eta Y(t-p) + \epsilon_{X,t}, \quad (5)$$

$$Y(t) = bY(t-1) + \epsilon_{Y,t}. \quad (6)$$

The parameters were set to be $a = 0.9$, $b = 0.9$ and coupling coefficient (η) was varied from $\eta = 0$ to $\eta = 1$ with step size = 0.1. Noise terms $\epsilon_{X,t} = \nu e_1$ and $\epsilon_{Y,t} = \nu e_2$ where e_1 and e_2 are sampled from the standard normal distribution and noise intensity $\nu = 0.03$. The process was simulated for $t = 1000$ time steps, with the first 500 transients discarded, resulting in a time series of length 2000 for both $X(t)$ and $Y(t)$. This procedure was repeated for $n = 1000$ trials

¹<https://webdav.tuebingen.mpg.de/cause-effect/>

for each value of the coupling coefficient. Figure 1 a, b, c and d represents the average (across 1000 trials for each coupling coefficient) LZ penalty from $X(t)$ to $Y(t)$ and $Y(t)$ to $X(t)$ averaged across 1000 independent random trials for each coupling coefficient corresponding to AR-1, AR-5, AR-20 and AR-100 respectively. The error bars in the plot represents the standard deviation. The proposed measure captures the correction direction of causality from $Y(t)$ to $X(t)$.

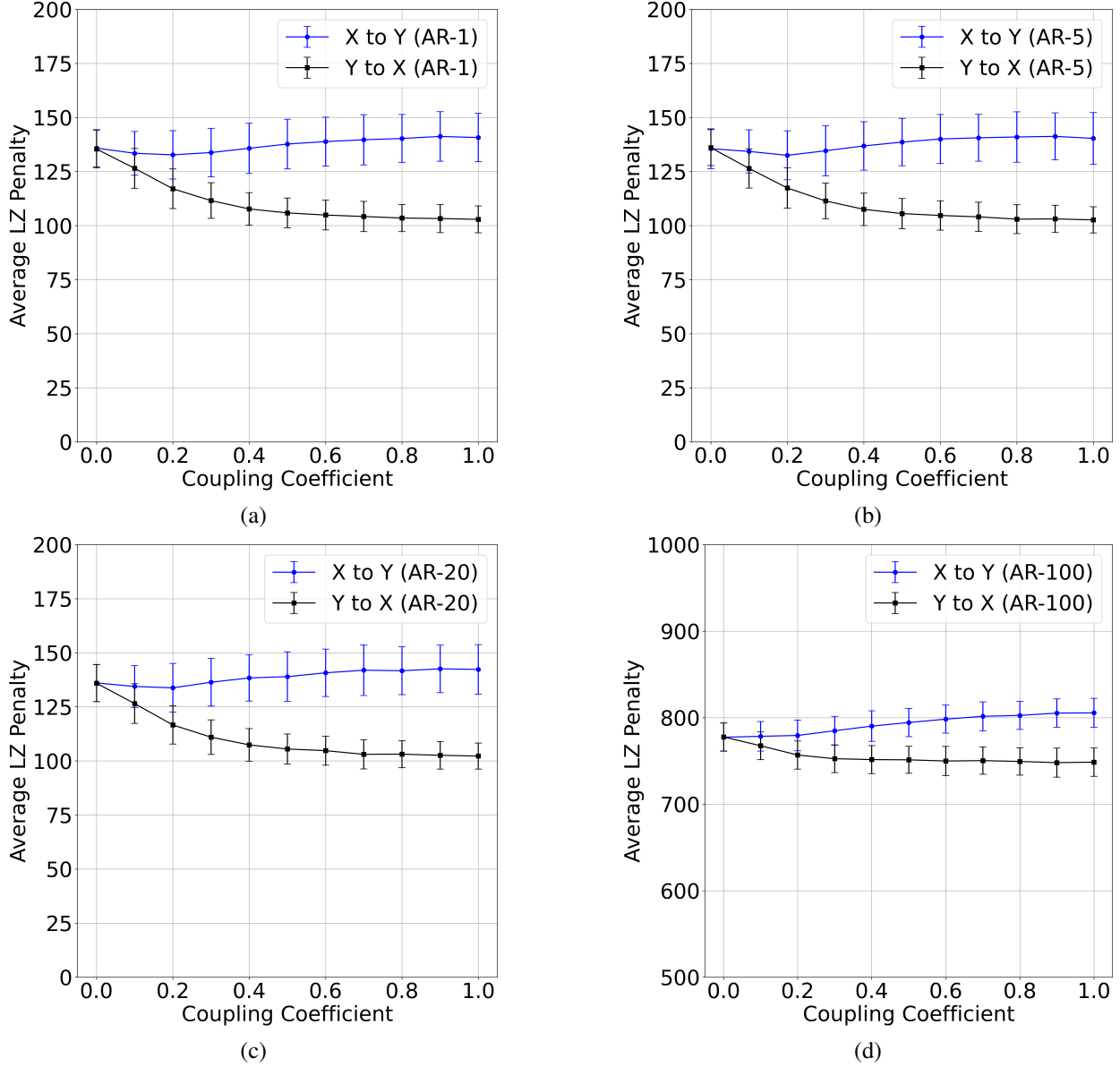


Figure 1: (a) Average LZ Penalty vs Coupling coefficients for AR-1 process. (b) Average LZ Penalty vs Coupling coefficients for AR-5 process. (c) Average LZ Penalty vs Coupling coefficients for AR-20 process. (d) Average LZ Penalty vs Coupling coefficients for AR-100 process. The coupling coefficients are varied from 0 to 1 with a step size of 0.1. For each coupling coefficient, LZ penalty was averaged across 1000 independent random trials.

2.2 Coupled Logistic Map

The 1D Logistic map is a chaotic map commonly used in population dynamics [13] study. The equations governing the dynamics of master-slave system of 1D Logistic map is as follows:

$$Y(t) = L_1(Y(t-1)), \quad (7)$$

$$X(t) = (1 - \eta)L_2(X(t-1)) + \eta Y(t-1). \quad (8)$$

The coupling coefficient η is varied from 0 to 0.9 with a step size of 0.1. $L_1(t) = A_1 \cdot L_1(t-1)(1 - L_1(t-1))$, and $L_2(t) = A_2 \cdot L_2(t-1)(1 - L_2(t-1))$, where $A_1 = 4$ and $A_2 = 3.82$.

For both systems, 1000 data instances ($Y(t)$ cause, $X(t)$ (effect)) are generated. Each of the data instances are of length 2000, after removing the initial 500 samples (transients) from the time series. Figure 2 represents the LZ penalty from $X(t)$ to $Y(t)$ and $Y(t)$ to $X(t)$ averaged across 1000 independent random trials for each coupling coefficient. We observe that the proposed measure correctly identifies the causal direction upto $\eta = 0.4$ as depicted in Figure 2 (a). From $\eta = 0.4$ onwards the timeseries $X(t)$ and $Y(t)$ are synchronized yielding to similar LZ penalty.

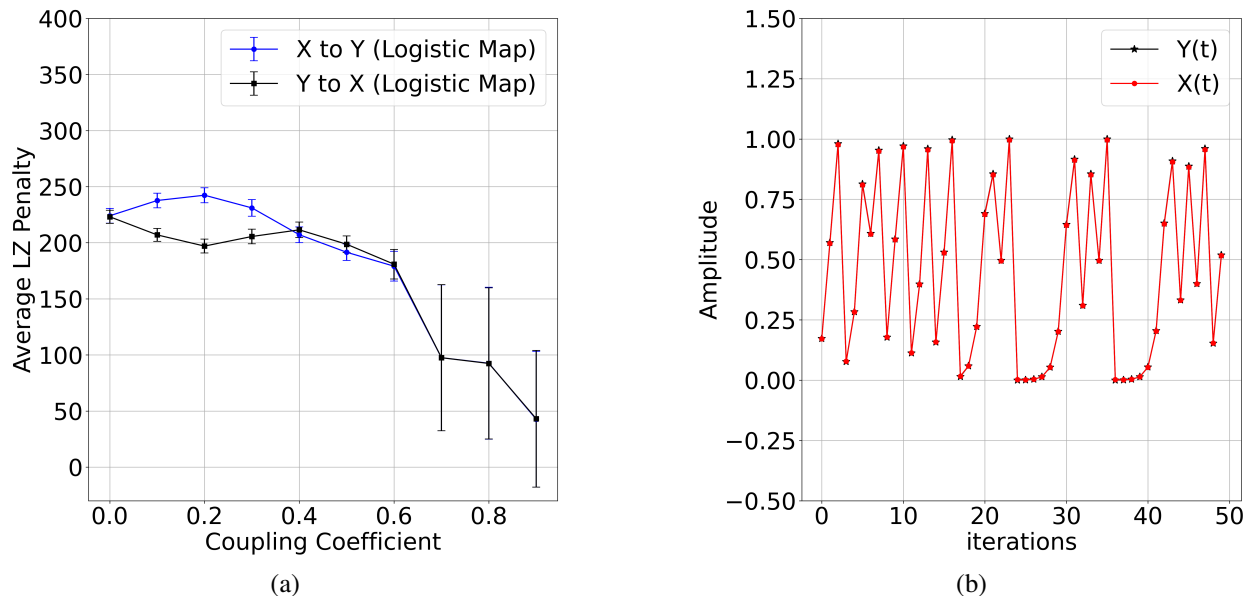


Figure 2: (a) LZ Penalty vs Coupling coefficients for coupled chaotic logistic map averaged across 1000 independent trials for each coupling coefficient. The coupling coefficients are varied from 0 to 0.9 with a step size of 0.1. (b) An instance of the timeseries $X(t)$ and $Y(t)$ for coupling coefficient $\eta = 0.4$ for first 50 iterations, indicating synchronization between $X(t)$ and $Y(t)$.

2.3 Tuebingen Cause Effect Pairs

Tuebingen data [11], [14] consists of 108 cause effect pairs. Out of which, we conducted our experiments on 104 cause-effect pairs. For each cause effect pairs, the ground truth is provided. There are only two variables indicated as X and Y . We use this data to determine whether $X \rightarrow Y$ or $Y \rightarrow X$ using the proposed LZ penalty measure. We evaluate the efficacy of the problem in determining the causal direction by comparing with the given ground truth. We use macro F1-score and accuracy to evaluate the proposed measure's performance. In our experiments, we obtain a macro F1-score = 0.44, accuracy = 50.8%. The top $k\%$ of pairs based on strength of causation is taken for $k = 1$ to $k = 100$, with a step size of 1. Figure 3 provides the accuracy vs decision rate ($k\%$) of the proposed LZ Penalty measure in comparison with $LZ - P$ measure defined in [10] (Note: the proposed formulation in this research is completely different from the $LZ - P$ formulation defined in [10]). The research in [8] have reported an accuracy of approximately 58% for a selected 95 datasets from Tuebingen Cause-Effect data pairs.

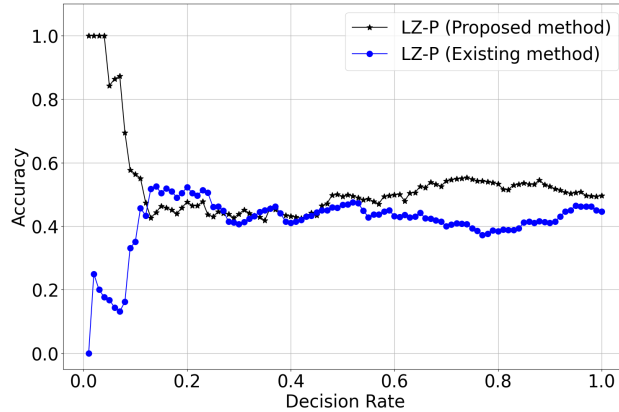


Figure 3: Accuracy vs. Decision rates for Tuebingen dataset using proposed LZ Penalty measure and LZ-P measure defined in [10].

2.4 Incorporation of the proposed causal and distance based measure in decision tree

In this section, we compare the performance evaluation of the proposed decision tree using *LZ* based causality measure, *LZ* based distance metric with Decision tree using gini impurity. The dataset used and their train-test distribution are provided in Table 1.

Table 1: Train-test split information for each dataset. 80%-20% train-test ratio was utilized. Imbalance Ratio is defined as the ratio of number of training samples in the most commonly occurring class to the number of training samples in the least commonly occurring class. It is calculated for the training data.

Dataset	Classes	Features	Training samples /class	Testing samples /class	Imbalance Ratio of train data
Iris [15]; [16]	3	4	(39,37,44)	(11,13,6)	1.189
Breast Cancer Wisconsin [14]; [17]	2	30	(286,169)	(71,43)	1.692
Congressional Voting Records [14, 18]	2	16	(101, 84)	(23,14)	1.202
Car Evaluation [14]; [19]	4	6	(307, 55, 968, 52)	(77, 14, 242, 13)	18.615
KRKPA7 [14]; [20]	2	35	(1227, 1329)	(300, 340)	1.083
Mushroom [14]; [21]	2	22	(2783, 1732)	(705, 424)	1.607
Heart Disease [14]; [22]	5	13	(124, 45, 30, 28, 10)	(36, 9, 5, 7, 3)	12.4
Thyroid [14]; [23]	3	21	(93, 191, 3488)	(73, 177, 3178)	37.505
AR Dataset	2	1	(113, 127)	(25, 35)	1.123

2.4.1 Results and Discussion

This section describes the experimental results carried out to test the efficacy of LZ distance metric based decision tree and LZ causal metric based decision tree. We test the model's performance on the datasets described in Appendix section 4.2, along with a synthetic autoregressive causal dataset that we generate, termed as the AR dataset, This dataset has been synthetically generated to provide data where there is an underlying causal structure between the various training examples. 450 training samples of an AR(1) process were generated according to the following equations:

$$X(t) = aX(t-1) + \eta Y(t-1) + \epsilon_{X,t} \quad (9)$$

$$Y(t) = bY(t-1) + \epsilon_{Y,t} \quad (10)$$

Coupling coefficient (η) was set to be 0.7, and parameters were fixed as $a = 0.8$, $b = 0.8$. Initial values of X and Y were set to 0 and the noise terms $\epsilon_{X,t}$ and $\epsilon_{Y,t}$ were modeled as νe_1 and νe_2 where e_1 and e_2 were sampled from the standard normal distribution and the noise intensity $\nu=0.03$. The timeseries Y was taken to be the feature data. The timeseries X was taken as the target to be classified after equi-width binning. The first 150 transients were removed, and the remaining samples were used for classification.

The train-test split for the datasets is done as described in Table 1. The hyperparameter tuning for LZ distance metric based decision tree and LZ causal metric based decision tree of the aforementioned datasets are mentioned in Appendix section 4.3. The summary of the results of the two proposed models are highlighted in Table 4 in Appendix section 4.4, along with the performance of a decision tree that uses Gini impurity as the splitting criteria. The comparison between the three models is illustrated in Figure 4.

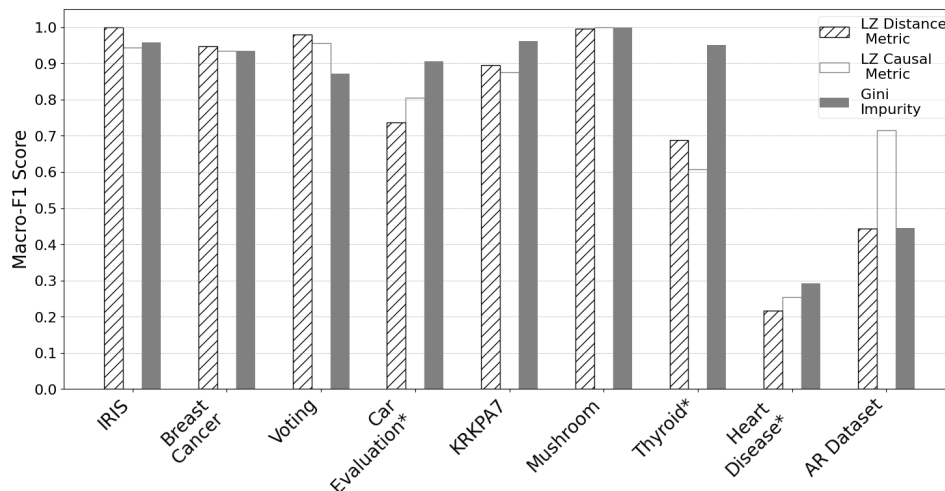
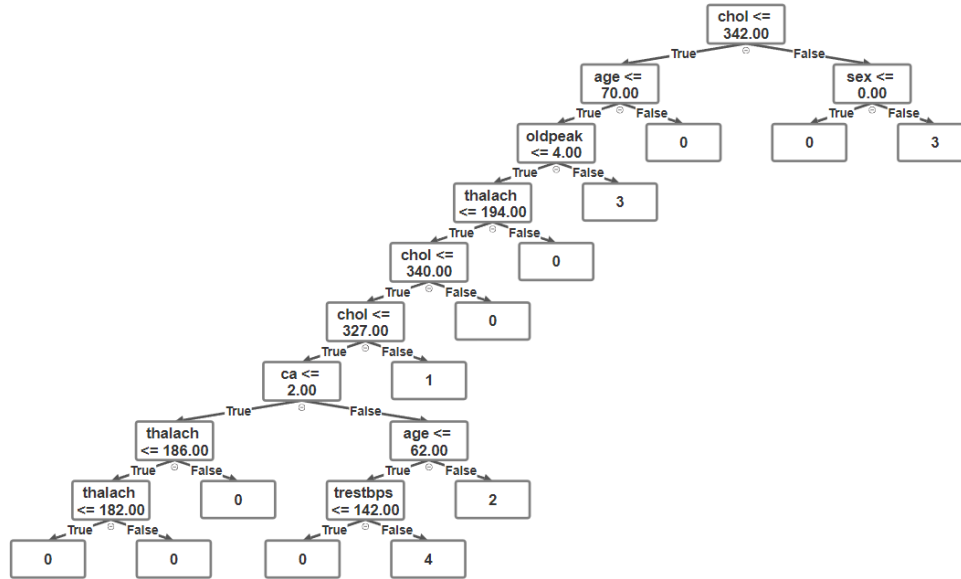


Figure 4: Bar Graph of macro F1 scores of predictions made by LZ distance metric based decision trees, LZ causal metric based decision trees and Gini impurity based decision trees, for various datasets. The datasets marked with a '*' are highly imbalanced.

The macro F1 scores obtained by the three models are comparable across most balanced datasets. The macro F1 score of the LZ -causal metric based decision tree on the AR dataset is 60.5% higher than both the macro F1 scores obtained by the other two algorithms on the same dataset. This result suggests that the causal decision tree effectively captures the intrinsic causal and temporal structures within the data, outperforming other models in discerning these underlying relationships. The Gini-entropy based decision tree significantly outperforms the Lempel Ziv complexity based models when the data is imbalanced, as seen in the Thyroid and Car evaluation datasets.

Table 2 and Table 5 (Appendix Section 4.6) illustrate the ranking for features on the Heart Disease and Mushroom datasets respectively.

The limitations of this research are highlighted in Appendix Section 4.7. We consider this as an opportunity to further develop the proposed method.



Abbreviations used: *chol*-Serum Cholesterol in mg/dl, *oldpeak*-ST depression induced by exercise relative to rest, *thalach*-Maximum heart rate achieved, *ca*-Number of major vessels (0-3) colored by fluoroscopy, *trestbps*-Resting blood pressure.

Figure 5: Causal Decision Tree for *Heart Disease* dataset.

Table 2: Ranking of Features of the Heart Disease dataset based on Causal Strength to the presence of heart disease.

Feature	Causal Strength
Serum Cholesterol in mg/dl	0.4361
Age	0.2025
Sex	0.1994
ST depression induced by exercise relative to rest	0.0997
Maximum heart rate achieved	0.0545
Number of major vessels (0-3) colored by fluoroscopy	0.0062
Resting blood pressure	0.0016

3 Conclusion

In this research, we propose a novel causality testing measure and distance metric based Lempel-Ziv complexity. Using the causality based measure, we were able to successfully capture the direction of causation of coupled AR processes and coupled logistic maps. We then incorporated the *LZ* based causality measure in decision trees to build trees that makes use of a causally informed splitting criteria. The efficacy of *LZ* distance metric based decision tree was also evaluated in the research experiments. We further provide a metric to analyze the feature importance based on causal strength derived from the *LZ* based causal decision tree. In future work, we will test the efficacy of the model on temporal causal data. We also plan to explore the applicability of the proposed distance metric based on Lempel-Ziv complexity in the bio-informatics domain, where order of nucleotide sequence plays a role.

References

- [1] Luca Longo, Mario Brcic, Federico Cabitza, Jaesik Choi, Roberto Confalonieri, Javier Del Ser, Riccardo Guidotti, Yoichi Hayashi, Francisco Herrera, Andreas Holzinger, et al. Explainable artificial intelligence (xai) 2.0: A manifesto of open challenges and interdisciplinary research directions. *Information Fusion*, 106:102301, 2024.
- [2] Harald O Stolberg, Geoffrey Norman, and Isabelle Trop. Randomized controlled trials. *American Journal of Roentgenology*, 183(6):1539–1544, 2004.
- [3] Clive WJ Granger. Investigating causal relations by econometric models and cross-spectral methods. *Econometrica: journal of the Econometric Society*, pages 424–438, 1969.
- [4] Thomas Schreiber. Measuring information transfer. *Physical review letters*, 85(2):461, 2000.

- [5] Norbert Wiener. The theory of prediction. *Modern mathematics for engineers*, 1956.
- [6] Aditi Kathpalia and Nithin Nagaraj. Measuring causality: The science of cause and effect. *Resonance*, 26:191–210, 2021.
- [7] Aditi Kathpalia and Nithin Nagaraj. Data-based intervention approach for complexity-causality measure. *PeerJ Computer Science*, 5:e196, 2019.
- [8] Kailash Budhathoki and Jilles Vreeken. Origo: causal inference by compression. *Knowledge and Information Systems*, 56(2):285–307, 2018.
- [9] Jilles Vreeken. Causal inference by direction of information. pages 909–917, 2015.
- [10] SY Pranay and Nithin Nagaraj. Causal discovery using compression-complexity measures. *Journal of Biomedical Informatics*, 117:103724, 2021.
- [11] Joris M Mooij, Jonas Peters, Dominik Janzing, Jakob Zscheischler, and Bernhard Schölkopf. Distinguishing cause from effect using observational data: methods and benchmarks. *Journal of Machine Learning Research*, 17(32):1–102, 2016.
- [12] Khalid Sayood. *Introduction to data compression*. Morgan Kaufmann, 2017.
- [13] Robert M May. Simple mathematical models with very complicated dynamics. *Nature*, 261(5560):459–467, 1976.
- [14] Markelle Kelly, Rachel Longjohn, and Kolby Nottingham. The UCI machine learning repository. <https://archive.ics.uci.edu>.
- [15] F. Pedregosa, G. Varoquaux, A. Gramfort, V. Michel, B. Thirion, O. Grisel, M. Blondel, P. Prettenhofer, R. Weiss, V. Dubourg, J. Vanderplas, A. Passos, D. Cournapeau, M. Brucher, M. Perrot, and E. Duchesnay. Scikit-learn: Machine learning in Python. *Journal of Machine Learning Research*, 12:2825–2830, 2011.
- [16] R. A. Fisher. The use of multiple measurements in taxonomic problems. *Annals of Eugenics*, 7(2):179–188, 1936.
- [17] W Nick Street, William H Wolberg, and Olvi L Mangasarian. Nuclear feature extraction for breast tumor diagnosis. In *Biomedical image processing and biomedical visualization*, volume 1905, pages 861–870. SPIE, 1993.
- [18] Congressional Voting Records. UCI Machine Learning Repository, 1987. DOI: <https://doi.org/10.24432/C5C01P>.
- [19] Marko Bohanec. Car Evaluation. UCI Machine Learning Repository, 1988. DOI: <https://doi.org/10.24432/C5JP48>.
- [20] Alen Shapiro. Chess (King-Rook vs. King-Pawn). UCI Machine Learning Repository, 1983. DOI: <https://doi.org/10.24432/C5DK5C>.
- [21] Mushroom. UCI Machine Learning Repository, 1981. DOI: <https://doi.org/10.24432/C5959T>.
- [22] Janosi, Andras, Steinbrunn, William, Pfisterer, Matthias, and Detrano, Robert. Heart Disease. UCI Machine Learning Repository, 1989. DOI: <https://doi.org/10.24432/C52P4X>.
- [23] Ross Quinlan. Thyroid Disease. UCI Machine Learning Repository, 1986. DOI: <https://doi.org/10.24432/C5D010>.

4 Appendix

4.1 Appendix A: Proof of $d_{LZ}(G_x, G_y)$ being a distance metric

The proof of $d_{LZ}(G_x, G_y)$ being a distance metric is as follows.

Consider two strings x and y . Let G_x and G_y be the grammar encoded by the LZ complexity algorithm for x and y respectively.

Definition of the Distance Function

Let G_x and G_y be two sets. Define the distance between them as:

$$d_{LZ}(X, Y) = |G_x/G_y| + |G_y/G_x|$$

where $|A|$ denotes the cardinality (size) of a set A . We will show that $d_{LZ}(G_x, G_y)$ satisfies the four properties of a metric.

1. Non-Negativity

We need to show that $d_{LZ}(G_x, G_y) \geq 0$ for all sets G_x and G_y .

By definition, G_x/G_y and G_y/G_x are both sets, and the cardinality of any set is non-negative. Hence:

$$|G_x/G_y| \geq 0 \quad \text{and} \quad |G_y/G_x| \geq 0$$

Thus,

$$d_{LZ}(G_x, G_y) = |G_x/G_y| + |G_y/G_x| \geq 0$$

Non-negativity is satisfied.

2. Identity of Indiscernibles

We must show that $d_{LZ}(G_x, G_y) = 0$ if and only if $G_x = G_y$.

If $G_x = G_y$: If $G_x = G_y$, then:

$$G_x - G_y = \emptyset \quad \text{and} \quad G_y - G_x = \emptyset$$

Thus:

$$|G_x/G_y| = 0 \quad \text{and} \quad |G_y/G_x| = 0$$

Therefore, $d_{LZ}(G_x, G_y) = 0$.

If $d_{LZ}(G_x, G_y) = 0$: If $d_{LZ}(G_x, G_y) = 0$, then, as both are individually greater than or equal to zero:

$$|G_x/G_y| = 0 \quad \text{and} \quad |G_y/G_x| = 0$$

This implies that:

$$G_x - G_y = \emptyset \quad \text{and} \quad G_y - G_x = \emptyset$$

which means $G_x = G_y$.

Thus, identity of indiscernibles is satisfied.

3. Symmetry

We need to show that $d_{LZ}(G_x, G_y) = d_{LZ}(G_y, G_x)$.

By the definition of set difference:

$$G_x/G_y = \{x \in G_x \mid x \notin G_y\}$$

and

$$G_y/G_x = \{y \in G_y \mid y \notin G_x\}$$

Therefore:

$$d_{LZ}(G_x, G_y) = |G_x/G_y| + |G_y/G_x|$$

and

$$d_{LZ}(G_y, G_x) = |G_y/G_x| + |G_x/G_y|$$

Since addition is commutative, we have:

$$d_{LZ}(G_x, G_y) = d_{LZ}(G_y, G_x)$$

Thus, symmetry is satisfied.

4. Triangle Inequality

We need to show that for any sets G_x , G_y , and G_z :

$$d_{LZ}(G_x, G_z) \leq d_{LZ}(G_x, G_y) + d_{LZ}(G_y, G_z)$$

This is equivalent to showing:

$$|G_x/G_z| + |G_z/G_x| \leq (|G_x/G_y| + |G_y/G_x|) + (|G_y/G_z| + |G_z/G_y|)$$

Consider some element in the set G_x/G_z . It either belongs to G_x/G_y , or G_y/G_z . This is true for every element in the set. Therefore, we have:

$$|G_x/G_z| \leq |G_x/G_y| + |G_y/G_z|$$

and similarly, for G_z/G_x ,

$$|G_z/G_x| \leq |G_z/G_y| + |G_y/G_x|$$

Adding these inequalities gives:

$$|G_x/G_z| + |G_z/G_x| \leq (|G_x/G_y| + |G_y/G_x|) + (|G_y/G_z| + |G_z/G_y|)$$

Thus, the triangle inequality is satisfied.

Conclusion

Since $d_{LZ}(G_x, G_y)$ satisfies non-negativity, identity of indiscernibles, symmetry, and the triangle inequality, it is a valid distance metric on the space of set of all sets.

4.2 Appendix B: Datasets

1. IRIS:

This dataset consists of 150 instances. There are three labels corresponding to three different types of irises', namely 'setosa', 'versicolour' and 'virginica'. The features describe the sepal length, sepal width, petal length and petal width measured in centimeters.

2. Breast Cancer Wisconsin

This dataset contains features derived from cell images to classify breast cancer as either benign or malignant. There are 569 samples with 30 numerical features describing characteristics of cell nuclei.

3. Congressional Voting Dataset

This dataset contains the information of the votes of each U.S House of Representatives Congressman on 16 key issues. Each of the 435 training samples is labeled by party affiliation, 'republican' or 'democrat'.

4. Car Evaluation

A classification dataset with 1,728 instances that classify cars as unacceptable, acceptable, good, or very good based on six categorical attributes: buying price, maintenance cost, number of doors, capacity, size of luggage boot, and safety.

5. KRKPA7

This dataset, also known as "King-Rook-King-Pawn-Against-Seven", is a chess dataset with 3196 samples. The 35 attributes describe the chess board in an endgame, and the training samples are classified based on whether White can win.

6. Mushroom

The Mushroom dataset contains records for 8,124 mushrooms, each classified as edible or poisonous. The dataset has 22 categorical attributes describing physical characteristics like cap shape, color, and odor, across 23 different species.

7. Heart Disease

This dataset is used for predicting heart disease presence, with 303 samples and 13 features such as age, sex, cholesterol levels, and blood pressure. The label indicates disease presence (1,2,3,4) or absence (0).

8. Thyroid

The Thyroid dataset focuses on thyroid disease detection, with instances labeled for three classes: normal, hyperthyroid, and hypothyroid. There are 3772 training samples and 3428 testing samples, over 21 features.

4.3 Appendix C: Hyperparameter tuning

In this section, the hyperparameter tuning for LZ distance metric based decision tree and LZ causal metric based decision tree are elaborated. For LZ distance metric based decision tree, we used stratified five fold crossvalidation using random split. In the case of LZ causal metric based decision tree, as well as the Gini entropy based Decision tree, we used five fold crossvalidation using timeseries split. Table 3 provides the best hyperparameters obtained after crossvalidation experiments for LZ distance metric based decision tree and LZ causal metric based decision tree corresponding to the datasets considered in this research. Hyperparameter tuning was done taking a range of 1 to 10 for the minimum number of samples per node, with a step size of 1. Maximum depth of tree was taken from 1 to 20 with the step size of 1.

Table 3: Tuned Hyperparameters and Training Performance Metrics for LZ-Distance-Metric based Tree, LZ-Causal-Metric Based Tree and Gini Impurity Based Tree across datasets

Datasets		Min Samples	Max Depth	Average F1 score on train data	Variance of F1 Score
Iris	LZ Distance Metric	2	11	0.94	0.004
	LZ Causal Metric	9	6	0.89	0.016
	Gini Impurity	9	4	0.953	0.002
Breast Cancer Wisconsin	LZ Distance Metric	9	4	0.89	0.0006
	LZ Causal Metric	2	6	0.91	0.0007
	Gini Impurity	4	8	0.931	0.0008
Congressional Voting Dataset	LZ Distance Metric	7	4	0.930	0.002
	LZ Causal Metric	5	9	0.965	0.0001
	Gini Impurity	9	9	0.979	0.0002
Car Evaluation	LZ Distance Metric	2	14	0.66	0.005
	LZ Causal Metric	2	9	0.514	0.0004
	Gini Impurity	2	9	0.832	0.002
KRRPA7	LZ Distance Metric	2	18	0.90	0.0002
	LZ Causal Metric	4	9	0.862	0.002
	Gini Impurity	3	9	0.968	0.0*
Mushroom	LZ Distance Metric	9	9	1.0	0.0*
	LZ Causal Metric	9	9	0.992	0.0*
	Gini Impurity	9	7	1.0	0.0*
Heart Disease	LZ Distance Metric	6	19	0.226	0.0002
	LZ Causal Metric	6	9	0.26	0.009
	Gini Impurity	3	9	0.301	0.002
Thyroid	LZ Distance Metric	9	20	0.664	0.002
	LZ Causal Metric	5	9	0.642	0.0005
	Gini Impurity	2	5	0.966	0.001
AR Dataset	LZ Distance Metric	2	9	0.503	0.004
	LZ Causal Metric	2	6	0.70	0.008
	Gini Impurity	2	6	0.55	0.004

*Variance of the order of 10^{-5} or less which has been rounded off to 0.

4.4 Appendix D: Performance Metrics

This section contains the accuracies, F1 scores, precision score and recall score for LZ-Distance-Metric based Tree, LZ-Causal-Metric Based Tree and Gini-Entropy Based Tree across various datasets.

Table 4: Performance metrics for LZ-Distance-Metric based Tree, LZ-Causal-Metric Based Tree and Gini-Entropy Based Tree across datasets

Datasets	Algorithm	Accuracy	F1 Score	Precision	Recall
Iris	LZ Distance Metric based DT	1.0	1.0	1.0	1.0
	LZ Causal Metric based DT	0.933	0.943	0.956	0.939
	Gini Impurity based DT	0.967	0.958	0.978	0.944
Breast Cancer Wisconsin	LZ Distance Metric based DT	0.947	0.948	0.939	0.943
	LZ Causal Metric based DT	0.939	0.934	0.937	0.932
	Gini Impurity based DT	0.938	0.934	0.936	0.932
Congressional Voting Records	LZ Distance Metric based DT	0.979	0.979	0.979	0.979
	LZ Causal Metric based DT	0.957	0.957	0.96	0.958
	Gini Impurity based DT	0.872	0.871	0.896	0.875
Car Evaluation	LZ Distance Metric based DT	0.829	0.682	0.734	0.664
	LZ Causal Metric based DT	0.76	0.510	0.570	0.496
	Gini Impurity based DT	0.945	0.883	0.914	0.865
KRKPA7 (Chess)	LZ Distance Metric based DT	0.895	0.895	0.895	0.896
	LZ Causal Metric based DT	0.876	0.876	0.877	0.875
	Gini Impurity based DT	0.961	0.961	0.960	0.962
Mushroom	LZ Distance Metric based DT	0.996	0.996	0.995	0.997
	LZ Causal Metric based DT	1.0	1.0	1.0	1.0
	Gini Impurity based DT	1.0	1.0	1.0	1.0
Heart Disease	LZ Distance Metric based DT	0.567	0.217	0.210	0.235
	LZ Causal Metric based DT	0.617	0.254	0.325	0.263
	Gini Impurity based DT	0.55	0.292	0.293	0.308
Thyroid	LZ Distance Metric based DT	0.946	0.688	0.827	0.640
	LZ Causal Metric based DT	0.940	0.607	0.818	0.556
	Gini Impurity based DT	0.992	0.951	0.946	0.957
AR Dataset	LZ Distance Metric based DT	0.467	0.444	0.444	0.445
	LZ Causal Metric based DT	0.717	0.716	0.719	0.718
	Gini Impurity based DT	0.45	0.446	0.45	0.448

4.5 Appendix E: LZ Distance Metric based decision tree and Gini entropy based decision tree

The following section contains the LZ distance metric based decision tree and the Gini entropy based decision tree for the heart disease dataset, seen in Figure 6 and Figure 7 respectively.

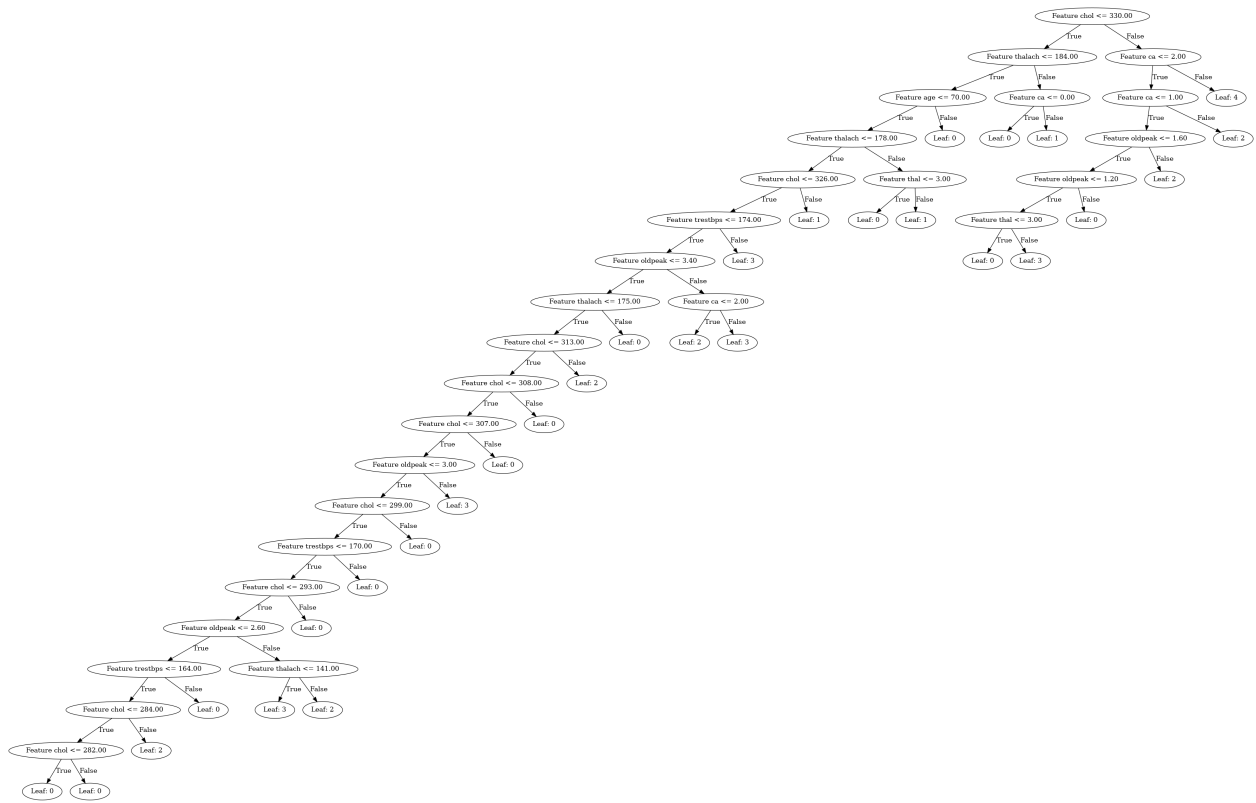


Figure 6: LZ Distance metric based decision tree generated for the heart disease dataset.

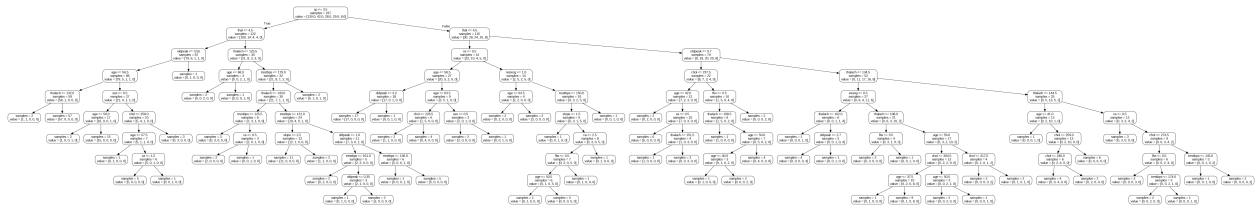


Figure 7: Gini Entropy based decision tree generated for the heart disease dataset.

4.6 Appendix F: Feature Ranking for Mushroom Dataset

This section contains the causal strength ranking for the features of the Mushroom dataset, seen in Table 5.

Table 5: Ranking of Features of the Mushroom dataset based on Causal Strength to whether the mushroom is poisonous.

Feature	Causal Strength
Odor	0.3181
Cap Surface	0.3041
Spore print color	0.2444
Ring Number	0.0374
Gill color	0.0374
Habitat	0.0187
Stalk color above ring	0.0187
Stalk surface above ring	0.0094
Stalk shape	0.0094
Cap colour	0.0023

4.7 Appendix G: Limitations

1. We consider an AR(1) process generated using the following equations:

$$X(t) = aX(t-1) + \eta Y(t-1) + \epsilon_{X,t} \quad (11)$$

$$Y(t) = bY(t-1) + \epsilon_{Y,t} \quad (12)$$

For a coupling coefficient $\eta = 0$, we found that the measure is sensitive to the parameter a (the coefficient of $X(t-1)$). We fixed the parameter $b = 0.6$ (the coefficient of $Y(t-1)$) and varied a from 0.1 to 0.9, with a step size of 0.1. When using 2 bins to generate the symbolic sequence, the measure showed a spurious causal relationship. We hypothesize that this may be due to the binned sequence failing to capture the underlying dynamics of the real-valued data, leading to arbitrary causal inferences. Figure 8 illustrates the sensitivity observed using the proposed measure.

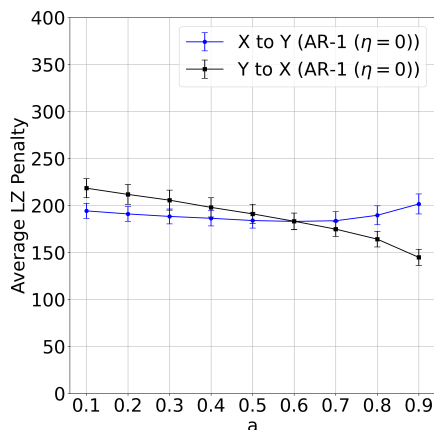


Figure 8: LZ Penalty vs. Coupling coefficient for the AR(1) process, averaged across 1000 independent trials with $\eta = 0$. The coefficient a (of $X(t-1)$) is varied from 0.1 to 0.9 in increments of 0.1.

2. The decision trees that utilises LZ based Causal Measure as well as the LZ-based distance metrics are unable to capture the dynamics of imbalanced data. This may occur as both algorithms minimize either the Lempel Ziv Penalty between the symbolic sequence representation of the feature and the symbolic sequence representation of the target or the edit distance between the grammar sets of the same. In case of data imbalance, it may achieve this minimization by collapsing the feature representation into a homogeneous sequence of zeros, or otherwise fail to capture the appropriate thresholding.
3. Validity of the proposed causal decision tree model: At present the validity of the proposed causal decision tree model relies on the interpretation of the domain expert. In the future work, we plan to investigate the notion of causal interpretability of the proposed decision tree model from an algorithmic point of view.

4.8 Appendix H: Code Availability

The python code used in this research are available in the following GitHub repository: <https://github.com/i-to-the-power-i/causal-lz-p-decision-tree>.